

Alexander Heinlein, Amanda A. Howard, Damien Beecroft, and Panos Stinis

# Multifidelity domain decomposition-based physics-informed neural networks for time-dependent problems

**Abstract:** Multiscale problems are challenging for neural network-based discretizations of differential equations, such as physics-informed neural networks (PINNs). This can be (partly) attributed to the so-called spectral bias of neural networks. To improve the performance of PINNs for time-dependent problems, a combination of multifidelity stacking PINNs and domain decomposition-based finite basis PINNs are employed. In particular, to learn the high-fidelity part of the multifidelity model, a domain decomposition in time is employed. The performance is investigated for a pendulum and a two-frequency problem as well as the Allen-Cahn equation. It can be observed that the domain decomposition approach clearly improves the PINN and stacking PINN approaches.

**Keywords:** Multifidelity, domain decomposition, physics-informed neural networks

**MSC2020:** 65M22, 65M55, 68T07

## 1 Introduction

Many problems arising in science and engineering exhibit a multiscale nature, with different processes taking place on various temporal and spatial scales. The solution of these problems is generally difficult for numerical methods. Multiscale methods have been developed to make numerical simulations of such problems feasible; examples are the multiscale finite element [12], homogeneous multiscale [9], generalized finite element [4] or variational multiscale [15] methods.

In recent years, inspired by the early work by Lagaris et al. [16], machine learning based techniques for the solution of partial differential equations (PDEs) have been developed. In this paper, we focus on physics-informed neural networks (PINNs) [23]; other methods, such as the Deep Ritz method [10], have

---

**Alexander Heinlein**, Delft University of Technology, Delft Institute of Applied Mathematics, 2628 CD Delft, Netherlands

**Amanda A. Howard, Panos Stinis**, Pacific Northwest National Laboratory, P.O. Box 999, Richland, WA, 99352, USA

**Damien Beecroft**, University of Washington, Seattle, WA, 98195, USA

been developed around the same time. Those methods have many potential advantages: they are easy to implement, allow for direct integration of data, and can be employed to solve inverse and high-dimensional problems. However, their convergence properties are not yet well-understood, and hence, the resulting accuracy is often limited. This can be partly accounted to the spectral bias of neural networks (NNs) [22], meaning that NNs tend to learn low frequency components of functions much faster than high frequency components. In multiscale problems, the high frequency components typically correspond to the fine scales, whereas the low frequency components correspond to the coarse scales. Therefore, multiscale problems are also particularly challenging to solve using PINNs.

In this paper, we aim at combining two techniques that have recently been developed to improve the training of PINNs in this context. On the one hand, we consider the multi-fidelity training approach introduced for PINNs [20] and extended to Deep Operator Networks (DeepONets, [17]) in [14, 18, 6]. In particular, we consider the approach of stacked PINNs [13] in which multiple networks are stacked on top of each other, such that models on top of the stack may learn those features that are not captured by the previous models. On the other hand, we employ multi-level Schwarz domain decomposition neural network architectures [8], which are based on the finite-basis PINNs (FBPINNs) [21] approach. In this approach, the learning of multiscale features is improved by localization. In particular, the network architecture is decomposed, such that the individual parts of the network learn features on the corresponding spatial or temporal scale. For an overview on the combination of domain decomposition approaches and machine learning, see, for instance, [11].

In related recent works, methods for iteratively training PINNs to progressively reduce the errors have been developed; see [1, 2, 3, 28]. These approaches, which vary in their implementation details, train each new network to reduce the residual from the previous network. In contrast, the work presented here trains for the entire solution at each iteration.

This paper is structured as follows: first, in Section 2, we describe the methodological framework. In particular, we first discuss PINNs in Section 2.1, then we describe multifidelity stacking PINNs in Section 2.2, as well as the domain decomposition approach in Section 2.3. Next, we introduce the specific domain decomposition in time employed in the model problems in Section 3. In Section 4, we present numerical results for several model problems, a pendulum and a two-frequency problem as well as the Allen-Cahn equation. We conclude with a brief discussion of the current and future work in Section 5. All training parameters used to generate the results are given in Table 1.

## 2 Methodology

### 2.1 Physics-informed neural networks

We consider a generic differential equation-based problem in residual form: find  $u$  such that

$$\begin{aligned} \mathcal{A}u &= 0 & \text{in } \Omega, \\ \mathcal{B}u &= 0 & \text{on } \partial\Omega, \end{aligned} \quad (1)$$

where  $\mathcal{A}$  is a differential operator and  $\mathcal{B}$  an operator for specifying the initial or boundary conditions. The solution  $u$  is defined on the domain  $\Omega$  and should have sufficient regularity to apply  $\mathcal{A}$  and  $\mathcal{B}$ . In order to solve eq. (1), we follow [16] and employ a collocation approach. In particular, we exploit that solving eq. (1) is equivalent to solving  $\arg \min_{\mathcal{B}u=0 \text{ on } \partial\Omega} \int_{\Omega} (\mathcal{A}u(\mathbf{x}))^2 d\mathbf{x}$ . We discretize the solution using a neural network  $\hat{u}(\mathbf{x}, \theta)$ , with parameters  $\theta$ , and the integral is approximated by the sum

$$\arg \min_{\mathcal{B}\hat{u}(\mathbf{x}, \theta)=0 \text{ on } \partial\Omega} \sum_{\mathbf{x}_i \in \Omega} (\mathcal{A}\hat{u}(\mathbf{x}_i, \theta))^2,$$

where the collocation points  $\mathbf{x}_i$  are sampled from  $\Omega$ . Different types of neural network architectures may be employed, and we will employ a combination of the approaches explained in sections 2.2 and 2.3.

The initial or boundary conditions in the second equation of eq. (1) can be enforced via hard or soft constraints. In the approach of hard constraints, they are explicitly implemented in the neural network function; cf. [16]. In this paper, we employ the approach of soft constraints instead, in which we incorporate the constraints into the loss function:

$$\arg \min_{\theta} \lambda_r \sum_{\mathbf{x}_i \in \Omega} (\mathcal{A}\hat{u}(\mathbf{x}_i, \theta))^2 + \lambda_{bc} \sum_{\mathbf{x}_i \in \partial\Omega} (\mathcal{B}\hat{u}(\mathbf{x}_i, \theta))^2 \quad (2)$$

Here,  $\lambda_r$  and  $\lambda_{bc}$  weight the residual of the differential equation and the initial and boundary conditions in the loss function. As discussed, for instance, in [26] an appropriate weighting is crucial for the convergence in optimizing eq. (2) using a gradient-based optimization method.  $\theta$  denotes all the trainable parameters in the network.

This approach has also been denoted as physics-informed neural networks (PINNs) in [23].

### 2.2 Multifidelity stacking PINNs

Multifidelity PINNs use two NNs to learn the correlation between low- and high-fidelity physics [20]. The goal is to train a linear network (with no activation function) to learn the linear correlation between the low- and high-fidelity

models, and a nonlinear network to learn the nonlinear correlation. By training a linear network, the resulting model is more expressive than just assuming that the correlation between the models is the identity. Moreover, under the assumption that the main part of the correlation is linear, separating the network into the linear and nonlinear parts allows for a smaller nonlinear network.

To train a multifidelity PINN we first train a standard single fidelity PINN  $\hat{u}^{SF}(\mathbf{x}, \theta^{SF})$ . In a second step, we then train a multifidelity network  $\hat{u}^{MF}$ , which consists of linear and nonlinear subnetworks that learn the correlation between the single fidelity PINN  $\hat{u}^{SF}(\mathbf{x}, \theta^{SF})$  and the solution:

$$\hat{u}^{MF}(\mathbf{x}, \theta^{MF}) = (1 - |\alpha|)\hat{u}_{linear}^{MF}(\mathbf{x}, \hat{u}^{SF}, \theta^{MF}) + |\alpha|\hat{u}_{nonlinear}^{MF}(\mathbf{x}, \hat{u}^{SF}, \theta^{MF}). \quad (3)$$

The linear network does not have activation functions, to force learning a linear correlation, and can be very small.  $\alpha$  is a trainable parameter to enforce maximizing the linear correlation.

The loss function in eq. (2) is modified to include the penalty  $\alpha^4$ :

$$\arg \min_{\theta} \lambda_r \sum_{\mathbf{x}_i \in \Omega} (\mathcal{A}\hat{u}(\mathbf{x}_i, \theta))^2 + \lambda_{bc} \sum_{\mathbf{x}_i \in \partial\Omega} (\mathcal{B}\hat{u}(\mathbf{x}_i, \theta))^2 + \lambda_{\alpha} \alpha^4 \quad (4)$$

In multifidelity stacking PINNs as presented in [13], multifidelity PINNs are trained recursively, each taking the output of the previously trained stacking layer as input. In this way, the previous layer serves as the low-fidelity model for the new stacking layer. The difference between [13] and the current work is that [13] does not consider domain decomposition, so each stacking layer has a single multifidelity PINN covering the entire domain. The approach considered here is more flexible and, as we will show in Section 4, results in smaller relative errors when trained on the same equations.

## 2.3 Domain decomposition-based neural network architectures

It has been observed in [21] that the high frequency components in the solution can be learned better if a domain decomposition is introduced into the PINN approach. To scale to larger numbers of subdomains, this approach has first been first extended to two-levels in [7] and then to an arbitrary number of levels in [8]. The general idea of the domain decomposition-based finite basis PINNs (FBPINNs) is to decompose the computational domain  $\Omega$  into  $J$  overlapping subdomains  $\Omega_j$ ,  $\Omega = \cup_{j=1}^J \Omega_j$ . As before,  $\Omega$  may be a space-time domain, and in this work we will focus on domain decomposition in time. On each subdomain, we define a space of network functions  $\mathcal{V}_j = \{\hat{u}_j(\mathbf{x}, \theta_j) | \mathbf{x} \in \Omega_j, \theta_j \in \Theta_j\}$ , where  $\hat{u}_j(\mathbf{x}, \theta_j)$  denotes a PINN model,  $\Theta_j = \mathbb{R}^{k_j}$  is the space of all trainable neural network parameters, and  $k_j$  is the number of network parameters.

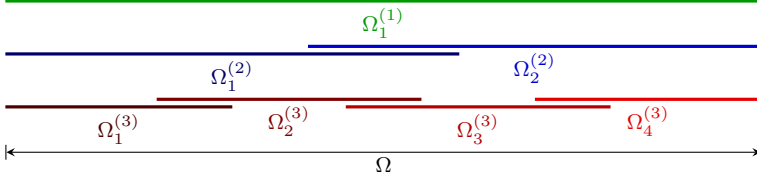


**Fig. 1:** Multilevel overlapping domain decomposition of  $\Omega$  with  $L = 3$  levels.

In order to represent the global solution of a given problem, we define window functions  $\omega_j$  with  $\text{supp}(\omega_j) \subset \Omega_j$  such that  $\{\omega_j\}_{j=1}^J$  form a partition of unity, that is,  $\sum_{j=1}^J \omega_j = 1$  on  $\Omega$ . Then, we can define a global neural network space  $\mathcal{V} = \sum_{j=1}^J \omega_j \mathcal{V}_j$ , and the global FBPINN function reads  $\hat{u}(\mathbf{x}, \theta) = \sum_{j=1}^J \omega_j \hat{u}_j(\mathbf{x}, \theta_j)$ . It has been observed that this approach may significantly improve the performance of PINNs; cf. [21]. However, similar to classical domain decomposition methods [25], the one-level approach is not scalable to large numbers of subdomains; see [7, 8].

To improve the scalability and the performance for multiscale problems, a hierarchy of domain decompositions may be employed. Define  $L$  levels of domain decompositions, with the overlapping domain decomposition at level  $l$  denoted by  $D^{(l)} = \{\Omega_j^{(l)}\}_{j=1}^{J^{(l)}}$ , where  $\Omega = \cup_{j=1}^{J^{(l)}} \Omega_j^{(l)}$  and  $J^{(l)}$  is the number of subdomains at level  $l$ ; cf. Figure 1. Even though there is generally no restriction on the overlapping domain decompositions, we choose  $J^{(1)} = 1$ , so the first level corresponds to a single global subdomain, and  $J^{(l)} < J^{(l+1)}$  for all  $l = 1, \dots, L$ .

Now, on each level  $l$  we define window functions  $\omega_j^{(l)}$  to be a partition of unity, so  $\sum_{j=1}^{J^{(l)}} \omega_j^{(l)} = 1$ , and  $\text{supp}(\omega_j^{(l)}) \subset \Omega_j^{(l)}$ . Similar to the one-level case, this yields the global neural network space  $\mathcal{V} = \sum_{l=1}^L \sum_{j=1}^{J^{(l)}} \omega_j^{(l)} \mathcal{V}_j^{(l)}$  and the global network function defined in terms of  $\theta = \cup_{l=1}^L \theta^{(l)}$  and  $\theta^{(l)} = \cup_{j=1}^{J^{(l)}} \theta_j^{(l)}$ :

$$\hat{u}(\mathbf{x}, \theta) = \frac{1}{L} \sum_{l=1}^L \hat{u}^{(l)}(\mathbf{x}, \theta^{(l)}) \quad \text{with} \quad \hat{u}^{(l)}(\mathbf{x}, \theta^{(l)}) = \sum_{j=1}^{J^{(l)}} \omega_j^{(l)} \hat{u}_j^{(l)}(\mathbf{x}, \theta_j^{(l)}). \quad (5)$$

It has been observed in [7, 8] that, due to increased communication between the subdomain models, the multilevel FBPINN approach may significantly improve the performance over the one-level approach.

## 2.4 Stacking FBPINNs

We combine the multifidelity stacking PINNs and the FBPINNs as follows: In the first level, we train a standard single fidelity PINN across the full domain

$\Omega^{(0)} = \Omega$ . Then, for each level  $l > 0$  we use a FBPINN network architecture modified to consist of multifidelity networks that takes as input the network from the previous level  $l - 1$ :

$$\hat{u}^{(l)}(\mathbf{x}, \theta^{(l)}) = \sum_{j=1}^{J^{(l)}} \omega_j^{(l)} \hat{u}_{j, MF}^{(l)}(\mathbf{x}, \hat{u}^{(l-1)}, \theta_j^{(l)}). \quad (6)$$

We note that Eq. (6) differs from Eq. (5) by a factor of  $1/L$ , because the output of FBPINNs is the sum of the networks trained at all levels, while the output of stacking FBPINNs is the sum of the networks for the final level. The networks at level  $l$  learn the correlation between the output of the  $l - 1$  level and the solution, and take as input the previously learned solution  $\hat{u}^{(l-1)}(\mathbf{x}, \theta^{(l-1)})$ :

$$\hat{u}_{j, MF}^{(l)}(\mathbf{x}, \theta_j^{(l)}) = (1 - |\alpha|) \hat{u}_{j, lin}^{(l)}(\mathbf{x}, \hat{u}^{(l-1)}, \theta_j^{(l)}) + |\alpha| \hat{u}_{j, nonlin}^{(l)}(\mathbf{x}, \hat{u}^{(l-1)}, \theta_j^{(l)}) \quad (7)$$

### 3 Domain decomposition in time

In this work, we are particularly interested in cases where classical PINNs fail to learn the temporal evolution, such as a damped pendulum and the Allen-Cahn equation. We consider a domain  $\Omega = \mathbf{X} \times [0, T]$  where  $\mathbf{X}$  denotes the spatial domain and  $T \in \mathbb{R}$ . Therefore, for the stacking FBPINN approach, we consider the domain decomposition in time:

$$\Omega_j^{(l)} = \left[ \frac{(j-1)T - \delta T/2}{J^{(l)} - 1}, \frac{(j-1)T + \delta T/2}{J^{(l)} - 1} \right]$$

where  $\delta > 1$  is the overlap ratio. For  $l = 0$ , we take  $\Omega_1^{(0)} = [0.5T - \delta T/2, 0.5T + \delta T/2]$ . The partition of unity functions are given by  $\omega_j^{(l)} = \frac{\hat{\omega}_j^{(l)}}{\sum_{j=1}^{J^{(l)}} \hat{\omega}_j^{(l)}}$ , where

$$\hat{\omega}_j^{(l)}(t) = \begin{cases} 1 & l = 0, \\ \left[ 1 + \cos\left(\pi(t - \mu_j^{(l)})/\sigma_j^{(l)}\right) \right]^2 & l > 0, \end{cases}$$

$\mu_j^{(l)} = T(j-1)/(J^{(l)} - 1)$ , and  $\sigma_j^{(l)} = (\delta T/2)/(J^{(l)} - 1)$ . For simplicity, we take  $J^{(l)} = 2^l$  in each case. An illustration of the window functions for  $T = 1$  and  $l = 2$  ( $J^{(2)} = 4$ ) is given in Figure 2.

As set up, each network only covers a small part of the time domain. To ease training, we scale the input in each domain to be in the range  $[-1, 1]$  by using a scaled time  $\hat{t} = t(l-1)/T - j$  as the input to network  $j$ . This scaling improves the robustness of the training.

In our applications we calculate the relative  $\ell_2$  error  $\frac{\|u(\mathbf{x}) - \hat{u}(\mathbf{x}, \theta)\|_2}{\|u(\mathbf{x})\|_2}$  where  $u$  denotes the exact solution and  $\hat{u}$  denotes the output from the multifidelity FBPINN.

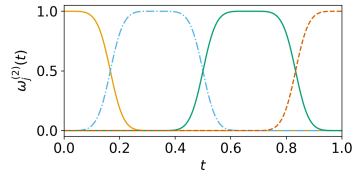


**Fig. 2:** Window functions  $\omega_j$  for  $l = 2$  and  $T = 1$ .

## 4 Results

### 4.1 Pendulum

While a relatively simple system, accurately training a PINN to predict the movement of a pendulum for long times presents challenges [27]. The pendulum movement is governed by a system of two first-order ODEs for  $t \in [0, T]$

$$\begin{aligned} \frac{ds_1}{dt} &= s_2, \\ \frac{ds_2}{dt} &= -\frac{b}{m}s_2 - \frac{g}{L}\sin(s_1), \end{aligned}$$

where  $s_1$  and  $s_2$  are the position and velocity of the pendulum, respectively. We employ the same parameters used in [27], that is,  $m = L = 1$ ,  $b = 0.05$ ,  $g = 9.81$ , and  $T = 20$ . We take  $s_1(0) = s_2(0) = 1$ . We compare the results with those for the stacking PINN from [13], which uses the same multifidelity architecture but only a single PINN on each level. As shown in Figure 3, the stacking FBPINN is able to reach a significantly lower relative  $\ell_2$  error. In addition, each network in the stacking FBPINN is significantly smaller than the networks used in the stacking PINN with the result that, at three stacking layers, the stacking FBPINN reaches a relative  $\ell_2$  error of 0.0074 with only 34 570 trainable parameters. In comparison, the best case stacking PINN from [13] requires four stacking levels to reach a relative  $\ell_2$  error of 0.0125 with 63 018 trainable parameters.

### 4.2 Multiscale problem

We now consider a toy model problem with a low and high frequency component, inspired by [21]:

$$\frac{ds}{dx} = \omega_1 \cos(\omega_1 x) + \omega_2 \cos(\omega_2 x), \quad (8)$$

$$s(0) = 0, \quad (9)$$

on domain  $\Omega = [0, 20]$  with  $\omega_1 = 1$  and  $\omega_2 = 15$ . The exact solution for this problem is  $s(x) = \sin(\omega_1 x) + \sin(\omega_2 x)$ .

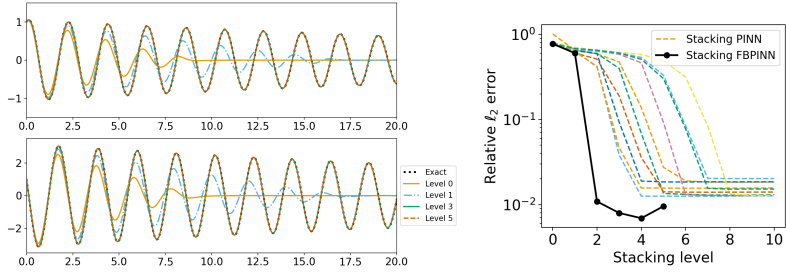


**Fig. 3:** Stacking FBPINN results for the pendulum problem: **Left:** Stacking FBPINN results for an illustrative example of  $s_1$  (top) and  $s_2$  (bottom) as a function of time for the pendulum problem up to five stacking FBPINN levels. **Right:** Pendulum relative  $\ell_2$  training errors comparing the work in the current paper (solid line) with the approach from [13] (dashed lines).

The results are shown in Figure 4. After two stacking levels, the stacking FBPINN reaches a relative  $\ell_2$  error of 0.00415, with 7822 trainable parameters. A comparable relative  $\ell_2$  error of 0.00612 is reached after 10 stacking levels with a stacking PINN with 11 179 trainable parameters. Also shown in Figure 4 (right) is the best case SF network from [13], which has a relative  $\ell_2$  error of 0.0949 with 16 833 trainable parameters. The stacking FBPINN outperforms the SF PINN with an error more than an order of magnitude lower, with less than half the trainable parameters. Additionally, the final stacking FBPINN reaches a relative  $\ell_2$  error of 0.00083, an order of magnitude lower than the final stacking PINN.

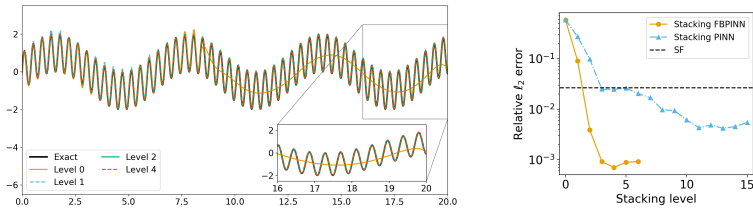


**Fig. 4:** Stacking FBPINN results for the multiscale problem: **Left:** Stacking FBPINN results for the single fidelity level 0 and the first four stacking FBPINN levels. **Right:** Multiscale relative  $\ell_2$  training errors comparing the work in the current paper with [13].



### 4.3 Allen-Cahn equation

Our third example is based on the Allen-Cahn equation and is given by

$$\begin{aligned}
 s_t - 0.0001s_{xx} + 5s^3 - 5s &= 0, & t \in (0, 1], x \in [-1, 1], \\
 s(x, 0) &= x^2 \cos(\pi x), & x \in [-1, 1], \\
 s(x, t) &= s(-x, t), & t \in [0, 1], x = -1, x = 1, \\
 s_x(x, t) &= s_x(-x, t), & t \in [0, 1], x = -1, x = 1.
 \end{aligned}$$

The Allen-Cahn equation presents difficulties for PINNs when attempting to learn the full solution from  $t = 0$  to 1 with a single PINN; see, e.g., [29, 19, 24].

We solve the Allen-Cahn equation by dividing the time domain into subdomains, as presented in section 3. The corresponding results for the stacking FBPINN are shown in Figure 5. The relative  $\ell_2$  error for applying two levels of the stacking FBPINN is 0.00594.

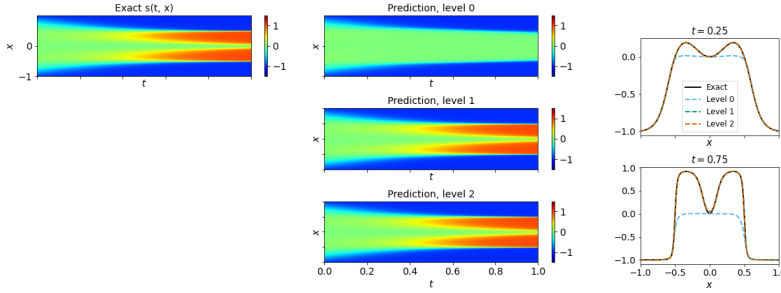


**Fig. 5:** Stacking FBPINN results for the Allen-Cahn equation. **Left:** Stacking FBPINN results for the single fidelity level 0 and the first two stacking FBPINN levels. **Right:** Line plots of the results from the stacking FBPINN at  $t = 0.25$  (top) and  $t = 0.75$  (bottom).

## 5 Discussion

In this paper, we have introduced the stacking FBPINN approach. For the considered time-dependent problems, it yielded more accurate results than stacking PINNs alone and, in some cases, it additionally required fewer total trainable parameters. This indicates that a domain decomposition in time can greatly improve the performance of stacking PINNs. In contrast to prior work on stacking PINNs, the stacking FBPINNs uses a sum of subdomain networks weighted by the partition of unity functions on the corresponding level. In contrast to multi-level FBPINNs in [8], in which the subdomain networks are summed across all

levels and trained simultaneously, the architecture and training of the stacking FBPINNs is sequential with respect to the levels; the idea is similar to multiplicative coupling as discussed in [7] but implemented differently using the stacking approach. This difference allows for stacking FBPINNs to consider different equations on different levels, akin to simulated annealing, as considered in [13], or to consider different physical models at different length scales. We leave this for future work.

## 6 Acknowledgments

This project was completed with support from the U.S. Department of Energy, Advanced Scientific Computing Research program, under the Scalable, Efficient and Accelerated Causal Reasoning Operators, Graphs and Spikes for Earth and Embedded Systems (SEA-CROGS) project (Project No. 80278). Pacific Northwest National Laboratory (PNNL) is a multi-program national laboratory operated for the U.S. Department of Energy (DOE) by Battelle Memorial Institute under Contract No. DE-AC05-76RL01830. The computational work was performed using PNNL Institutional Computing.

## 7 Training parameters

	Section 4.1	Section 4.2	Section 4.3
<b>Level 0 learning rate &amp; decay rate</b>	$5 \times 10^{-3}, 0.99$	$10^{-3}, 0.99$	$10^{-4}, 0.99$
<b>Level 0 network width</b>	100	32	100
<b>Level 0 network layers</b>	3	3	6
<b>Level 0 iterations</b>	200 000	200 000	200 000
<b>Nonlinear network width</b>	32	16	200
<b>Nonlinear network layers</b>	3	4	4
<b>Linear network size</b>	[2, 4, 2]	[1, 5, 1]	[1, 5, 1]
<b>MF learning rate &amp; decay rate</b>	$5 \times 10^{-3}, 0.99$	$5 \times 10^{-3}, 0.95$	$5 \times 10^{-3}, 0.95$
<b>BC batch size</b>	1	1	128
<b>Residual batch size</b>	400	400	1024
<b>Iterations</b>	200 000	300 000	300 000
$\lambda_r, \lambda_{bc}, \lambda_\alpha$	1.0, 1.0, 1.0	10.0, 1.0, 1.0	10.0, 1.0, $10^{-5}$

**Tab. 1:** Training parameters for the results in the paper. The learning rate is set using the exponential\_decay function in Jax [5] with the given learning rate and decay rate and 2000 decay steps. The training parameters used for the stacking PINN results are given in [13].

# Bibliography

- [1] M. Ainsworth and J. Dong. Galerkin neural networks: A framework for approximating variational equations with error control. *SIAM J. Sci. Comput.*, 43(4):A2474–A2501, 2021.
- [2] Mark Ainsworth and Justin Dong. Galerkin neural network approximation of singularly-perturbed elliptic systems. *Comput. Methods Appl. Mech. Eng.*, 402:115169, 2022.
- [3] Z. Aldirany, R. Cottreau, M. Laforest, and S. Prudhomme. Multi-level neural networks for accurate solutions of boundary-value problems. *arXiv:2308.11503*, 2023.
- [4] I. Babuška and J. E. Osborn. Generalized Finite Element Methods: Their Performance and Their Relation to Mixed Methods. *SIAM J. Numer. Anal.*, 20(3):510–536, June 1983.
- [5] J. Bradbury, R. Frostig, P. Hawkins, M. J. Johnson, C. Leary, D. Maclaurin, G. Necula, A. Paszke, J. VanderPlas, S. Wanderman-Milne, and Q. Zhang. JAX: composable transformations of Python+NumPy programs, 2018.
- [6] S. De, M. Reynolds, M. Hassanaly, R. N. King, and A. Doostan. Bi-fidelity modeling of uncertain and partially unknown systems using deeponeets. *arXiv:2204.00997*, 2022.
- [7] V. Dolean, A. Heinlein, S. Mishra, and B. Moseley. Finite basis physics-informed neural networks as a Schwarz domain decomposition method, November 2022. *arXiv:2211.05560*.
- [8] V. Dolean, A. Heinlein, S. Mishra, and B. Moseley. Multilevel domain decomposition-based architectures for physics-informed neural networks, June 2023. *arXiv:2306.05486* [cs, math].
- [9] W. E, B. Engquist, X. Li, W. Ren, and E. Vanden-Eijnden. Heterogeneous multiscale methods: A review. *Commun. Comput. Phys.*, 2(3):367–450, June 2007.
- [10] W. E and B. Yu. The Deep Ritz Method: A Deep Learning-Based Numerical Algorithm for Solving Variational Problems. *Commun. Math. Stat.*, 6(1):1–12, March 2018.
- [11] A. Heinlein, A. Klawonn, M. Lanser, and J. Weber. Combining machine learning and domain decomposition methods for the solution of partial differential equations — a review. *GAMM-Mitteilungen*, 44(1):Paper No. e202100001, 28, 2021.
- [12] T. Y. Hou and Y. Efendiev. *Multiscale Finite Element Methods: Theory and Applications*. Springer, New York, NY, 2009.
- [13] A. A. Howard, S. H. Murphy, S. E. Ahmed, and P. Stinis. Stacked networks improve physics-informed training: applications to neural networks and deep operator networks, November 2023. *arXiv:2311.06483*.
- [14] A. A. Howard, M. Perego, G. E. Karniadakis, and P. Stinis. Multifidelity deep operator networks for data-driven and physics-informed problems. *J. Comput. Phys.*, 493:112462, November 2023.
- [15] T. J. R. Hughes. Multiscale phenomena: Green’s functions, the Dirichlet-to-Neumann formulation, subgrid scale models, bubbles and the origins of stabilized methods. *Comput. Methods Appl. Mech. Eng.*, 127(1):387–401, November 1995.
- [16] I.E. Lagaris, A. Likas, and D.I. Fotiadis. Artificial neural networks for solving ordinary and partial differential equations. *IEEE Trans. Neural Networks*, 9(5):987–1000, September 1998. Conference Name: IEEE Transactions on Neural Networks.
- [17] L. Lu, P. Jin, and G. E. Karniadakis. DeepONet: Learning nonlinear operators for identifying differential equations based on the universal approximation theorem of operators. *Nat. Mach. Intell.*, 3(3):218–229, March 2021. *arXiv:1910.03193*.
- [18] L. Lu, R. Pestourie, S. G. Johnson, and G. Romano. Multifidelity deep neural operators for efficient learning of partial differential equations with application to fast inverse design of nanoscale heat transport. *Phys. Rev. Res.*, 4(2):023210, 2022.
- [19] R. Matthey and S. Ghosh. A novel sequential method to train physics informed neural net-

- works for Allen Cahn and Cahn Hilliard equations. *Comput. Methods Appl. Mech. Eng.*, 390:114474, 2022.
- [20] X. Meng and G. E. Karniadakis. A composite neural network that learns from multi-fidelity data: Application to function approximation and inverse PDE problems. *J. Comput. Phys.*, 401:109020, 2020.
- [21] B. Moseley, A. Markham, and T. Nissen-Meyer. Finite basis physics-informed neural networks (FBPINNs): a scalable domain decomposition approach for solving differential equations. *Adv. Comput. Math.*, 49(4):62, July 2023.
- [22] N. Rahaman, A. Baratin, D. Arpit, F. Draxler, M. Lin, F. A. Hamprecht, Y. Bengio, and A. Courville. On the Spectral Bias of Neural Networks, May 2019. [arXiv:1806.08734](https://arxiv.org/abs/1806.08734).
- [23] M. Raissi, P. Perdikaris, and G. E. Karniadakis. Physics-informed neural networks: a deep learning framework for solving forward and inverse problems involving nonlinear partial differential equations. *J. Comput. Phys.*, 378:686–707, 2019.
- [24] F. M. Rohrhofer, S. Posch, C. Gößnitzer, and B. C. Geiger. On the role of fixed points of dynamical systems in training physics-informed neural networks. [arXiv:2203.13648](https://arxiv.org/abs/2203.13648), 2022.
- [25] A. Toselli and O. Widlund. *Domain decomposition methods — algorithms and theory*, volume 34 of *Springer Series in Computational Mathematics*. Springer-Verlag, Berlin, 2005.
- [26] S. Wang, X. Yu, and P. Perdikaris. When and why PINNs fail to train: A neural tangent kernel perspective. *J. Comput. Phys.*, 449:110768, January 2022.
- [27] Sifan Wang and Paris Perdikaris. Long-time integration of parametric evolution equations with physics-informed DeepONets. *J. Comput. Phys.*, 475:111855, 2023.
- [28] Y. Wang and C.-Y. Lai. Multi-stage neural networks: Function approximator of machine precision. [arXiv:2307.08934](https://arxiv.org/abs/2307.08934), 2023.
- [29] C. L. Wight and J. Zhao. Solving Allen-Cahn and Cahn-Hilliard equations using the adaptive physics informed neural networks. [arXiv:2007.04542](https://arxiv.org/abs/2007.04542), 2020.